A Survey of Current Developments in Surface Tension Devices for Propellant Acquisition

S. C. De Brock, R. K. Grove, and R. O. Sloma
Lockheed Missiles & Space Company, Sunnyvale, Calif.

AND

D. L. Balzer, and Yvonne Brill
RCA, Princeton, N. J.

AND

G. A. Yankura
Jet Propulsion Laboratory, Pasadena, Calif.

THE task of a propellant expulsion system is to supply gas-free propellant on demand to spacecraft thrusters for the duration of the mission. For orbital spacecraft, which may experience periods of adverse or near zero-g accelerations, the expulsion system must assure that all or portions of the propellants are in contact with the tank outlet; that gas is prevented from entering the tank outlet during thruster startup; that pressurization gas entrained in the settling propellant bulk does not enter the tank outlet; and that propellant vortexing, gas pull-through, and propellant slosh do not significantly reduce the system expulsion efficiency.

Many types of positive propellant expulsion systems have been developed for orbital spacecraft, each with advantages and problems, as summarized in Table 1. Development of these devices usually centers on mechanical testing in simulated prototype environments. Although performance of these devices has been good, the reliability concern of the mission planner increases when very long missions are considered because there are no established accelerated life testing techniques. Recent experience with capillary systems has shown that they satisfy expulsion system requirements as well as the desire for passive simplicity. Indeed, the question of long

Mr. S. C. DeBrock joined Lockheed Missiles & Space Company (LMSC) in 1959 and is presently Manager of the Propulsion Systems Department with the Space Systems Division. He received B.S. degrees in Aeronautical Engineering and Engineering Math from the University of Michigan. He has been active in analysis, preliminary design, and development of advanced propulsion systems and equipment, particularly surface tension devices. He has published numerous papers on capillary propellant management systems and is currently Vice Chairman of the AIAA Propellant Expulsion Working Group. He is a member of AIAA.

Mr. R. K. Grove is a Senior Staff Engineer in the Propulsion Systems Department at LMSC His background includes 27 years of aeronautical design and analysis, including development of surface tension systems for the storage and feed of propellants in various spacecraft. Prior to joining Lockheed, he served with McDonnell Aircraft Co., the Atomic Energy Commission in Washington, D.C., the Packard Motor Car Co., and Continental Aviation and Engineering. He holds several patents related to airplanes, helicopters, gas turbines, turbojets, and the application of surface tension to propellant management.

Mr. R. O. Sloma is a Senior Research Engineer in the Propulsion Systems Department of LMSC, involved primarily with the analysis and development of propulsion systems for orbiting spacecraft. He has published a number of papers on capillary propellant management techniques. He received B.S. and M.S. degrees from Stanford University. He is a member of AIAA.

Mr. D. L. Balzer joined RCA-AED in February 1970 as Manager, Propulsion Systems, responsible for the Division's propulsion activities. Earlier he was with Martin Marietta Denver Division as Program Manager of two NASA study contracts on propellant management, and with the Rocketdyne Division of North American Rockwell. He received a B.S. degree in Chemical Engineering from Montana State University in 1958 and is a member of AIAA.

Miss Yvonne C. Brill joined the Advanced Development Division, RCA Astro-Electronics, Princeton, N.J., in 1966 and is responsible for analysis and design of spacecraft propulsion systems. She has worked on rockets, ramjets, and advanced turbojets at Wright Aeronautical, United Aircraft Research Labs., Marquardt, and the Rand Corporation. She holds an M.S. in chemistry from the University of Southern California and is Secretary of the AIAA Propellant Expulsion Working Group. He is a member of AIAA.

Mr. G. A. Yankura is a Senior Engineer in the Liquid Propulsion Section Feed System Development Group of the Jet Propulsion Laboratory. He is a member of the Mariner '71 midcourse correction propulsion system team and is engaged in development and testing of propellant expulsion devices. He received B.S. and M.S. degrees in Mechanical Engineering from the University of Southern California.

Presented as Paper 70-685 at the AIAA 6th Propulsion Joint Specialist Conference, San Diego, California, June 15–17, 1970; submitted July 6, 1970, revision received October 5, 1970.

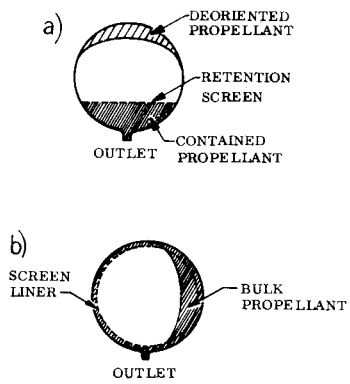

Fig. 1 a) Partial retention system; b) total communication system screen linear design.

life is reduced to the ability of the propellant tank shell itself to survive the mission from the standpoint of corrosion and gas evolution.

The first capillary propellant expulsion system was orbited about 6 years ago. Since then, there has been a steady growth in industry interest and experience with these systems. This survey highlights their principles of operation in relation to various expulsion requirements, analysis techniques for system design and operational behavior, methods of performance testing, materials compatibility and selection, methods of structural testing, and flight experience.

Capillary Propellant Management Concepts

Two basic approaches to capillary propellant management have evolved: 1) partial retention, and 2) total communication systems. Partial retention systems (Fig. 1a) retain only a limited quantity of propellant at the tank outlet and have essentially no control over the bulk propellant behavior. Capillary forces position enough propellant at the tank outlet to supply the engine during restart flow transients and to sustain flow until bulk propellant settling occurs. Partial retention devices are generally limited to unidirectional thrust applications, since they rely upon thrust to provide propellant settling; an exception might be an application where small volumes of propellant are withdrawn from the outlet reservoir to supply lateral thrusters followed by axial thruster firing to allow bulk propellant settling and refill of the retention device. A further restriction is that temperature gradients which tend to evaporate liquid propellant from the tank outlet and condense propellant vapor away from the outlet cannot be tolerated for sustained periods of time. Partial retention devices tend to be smaller, lighter and less costly than total communication devices, and they can be designed to withstand moderately high adverse accelerations. These advantages must be evaluated in light of the operational complexities of refilling the device after each engine firing.

Total communication devices (Fig. 1b) maintain communication from the tank outlet to the bulk propellant throughout the spacecraft operational life. They can be designed for either unidirectional or multidirectional thrust systems and place no refill constraints on the number or duration of engine firings. They impose essentially no limit on thermal gradients since the capillary communication elements replenish any evaporative losses at the outlet end of the tank. However, because they typically must retain propellant over the entire length of a tank, they are weaker propellant retainers, heavier, and more complex than the equivalent partial retention devices.

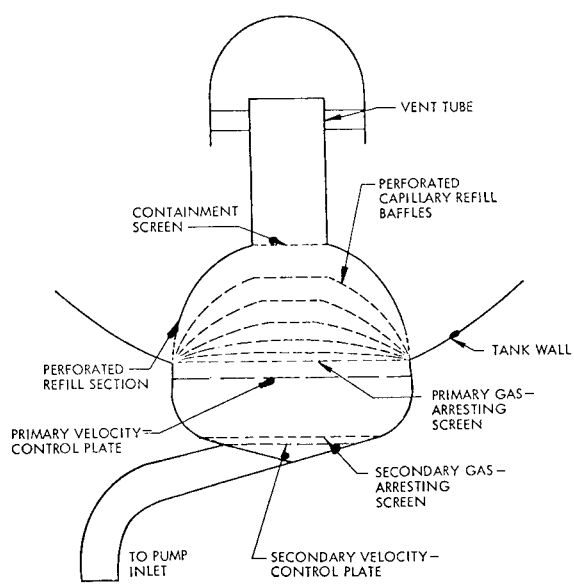

Fig. 2 Improved Agena design.

Partial Retention Designs

One of the earlier partial retention approaches[1] is the system used on the current Agena vehicle. The containment screens are sized to retain propellant against approximately 1-g negative and $\frac{1}{2}$-g lateral accelerations. Several seconds of high-g thrusting are needed to expel all gas from under the containment screen, and for this reason, the propellant management system normally allows only two or three engine starts with deoriented propellants. For those missions where propellant is oriented over the tank outlet at restart or the burns are long, there are no limitations on the number of restarts the

Table 1 Positive expulsion system comparison

Expulsion system	Strong points	Problem areas
Piston	Positive displacement; variable initial ullage gas volume	Heavy; leakage; jamming due to cocking or corrosion; limited to cylindrical tanks
Bladders	Much development and flight experience; adaptable to most tank geometries and initial gas ullage volume	Long term compatibility; gas permeation; poor expulsion efficiency; folding geometry conducive to pinhole leaks
Metallic bellows	Good compatibility; predictable performance adaptable to varying tank geometries and initial ullage volumes	High weight; cocking during expulsion; high Δp required for expulsion
Elastomeric diaphragm	Good expulsion efficiency; trouble free and repeatable diaphragm geometry during expulsion	Poor wear characteristics during prolonged propellant slosh; poor long life compatibility; limited to spherical tank geometry with significant initial ullage volume
Metallic diaphragm	Good compatibility; not sensitive to propellant slosh	Limited to spherical tank geometry; moderate ΔP required for expulsion
Rolling diaphragm	Good compatibility; not dependent on initial ullage volume	High ΔP, required for expulsion; limited to cylindrical tank geometry
Capillary systems	Variable initial ullage volumes and tank geometry; good compatibility and overall expulsion performance	Demonstration of expulsion performance with full-scale prototype units at 1-g is limited by capillary strength of propellants.

propellant management system can supply. The external sump arrangement is used to allow improved draining efficiency relative to an internally located device.

To extend the capability of the current Agena system to allow multiple burn operation without the need for minimum burn time requirements and to allow incorporation of an integral secondary propulsion system which also feeds from the main tanks, the Improved Agena design[2] shown in Fig. 2 was devised. Propellant retention is accomplished with screens at the top and around the base of the internal assembly, in a similar manner to the current Agena system operation. The nested semispherical baffles within the internal assembly provide tapered passages which provide a passive capillary filling action whenever propellant is brought into contact with the base of the internal assembly shell. The shielded vent tube allows refill to occur when the propellant management assembly is covered over with propellant. The graduated holes in the nested baffles, the gas arrester screen, and the velocity control plate combine to control the main engine start transient low-g surface dip and prevent gas ingestion into the outlet.

A simpler system is used on the Apollo.[3] Screens at the outlet end of each tank retain propellant over the outlet during coast periods against any adverse acceleration loads. Prior to engine start, propellant settling rockets position all propellant at the outlets, so the system serves primarily to keep gas out of the tank outlet during coast.

The capillary device used on Mariner '71 as a gas arresting system in the event of bladder gas permeation is shown in Fig. 3. If pressurization gas is present next to the device, it will be drawn into the first stage of the trap until liquid settles over the perforated surface of the device. During a series of short burns, additional gas will be taken in, but the internal perforated elements prevent it from reaching the outlet. During a longer burn, gas will be hydrostatically expelled from the device, allowing further operations of the propulsion system. The labyrinth passages and many geometric features are necessary because the tanks are loaded and boosted in an upside-down attitude and must tolerate large tilt angles.

Total Communication Approaches

In principle, the simplest design for total communication consists of lining a propellant tank with a screen or perforated sheet adjacent to the tank wall, as pictured in Fig. 1b. Typical examples of this approach[4] are the tanks used on the X-15 Flight Research Vehicle[5] and a number of drone missiles.

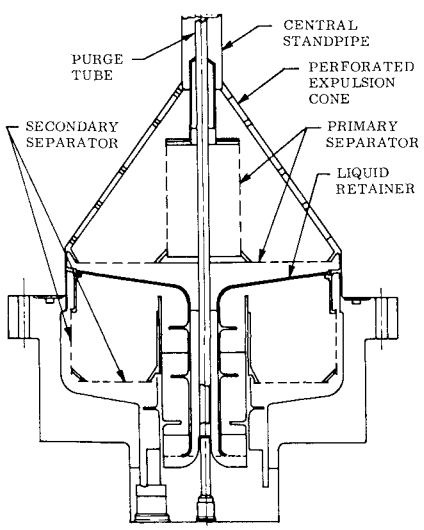

Fig. 3 Propellant standpipe and acquisition trap assembly.

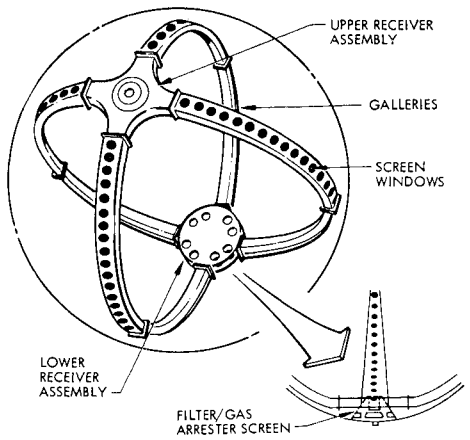

Fig. 4 62-in.-diam hydrazine tank design.

When the space between the tank wall and the liner is filled, the perforations keep the liner full against adverse accelerations while allowing communication from the tank outlet to any bulk propellant location on the wall of the tank.[6] Since all propellants on tank materials are good wetters (low contact angle), propellant will always be wall bound in a location dictated by the acceleration environment. Thrust or acceleration loads can be applied in any direction and propellant flows from the bulk puddle through the liner, along the annular wall-to-liner gap, and to the outlet. For tanks filled completely on the ground, the liner-wall gap is full at liftoff; when ullage volumes are present at liftoff, capillary action is relied upon to draw propellant into the gap after injection into a low-g acceleration environment.

For larger tanks where the weight of a complete liner becomes excessive, an alternative approach is to construct galleries which connect the outlet to possible propellant locations but do not communicate with the entire tank wall surface. An example of this is the 62-in.-diam spherical hydrazine tank design[7] shown in Fig. 4. This tank is placed in orbit approximately half-full. The galleries fill by capillary action after injection, and communication to the outlet is provided throughout the mission.

A cross-baffle design (Fig. 5), well suited for very low-g applications, is being evaluated for use in the Viking orbiter tanks. In a low-g field, propellant location and surface shape are dictated by the geometry of the baffles. The design shown has tapered baffles which bias the propellant over the tank outlet but still provide communication from the outlet to all other portions of the tank. As acceleration loads

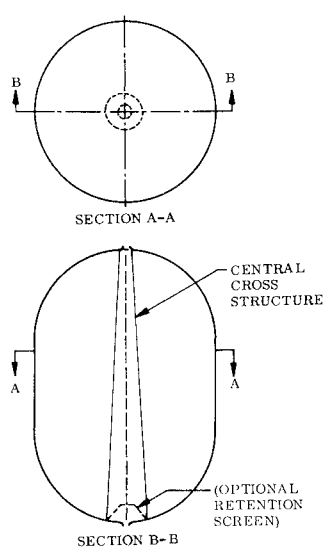

Fig. 5 LRC/JPL cross baffle concept.

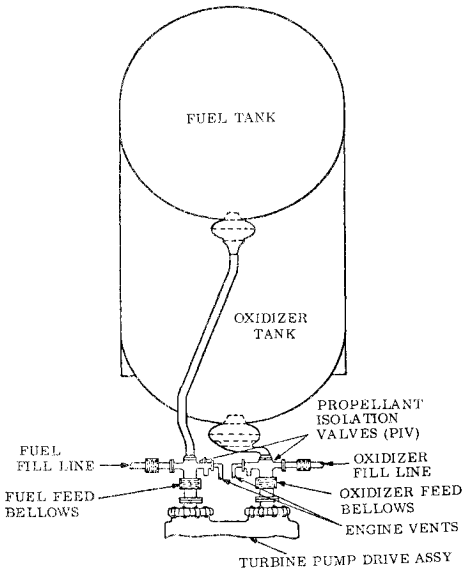

Fig. 6 Current Agena system.

increase, the number of baffles can be increased; the only limitation on capillary strength is the ability to construct devices with large numbers of baffles and the weight penalties which may result. To permit propellant feed to the outlet during lateral acceleration, the baffles can be extended to the walls of the tank; the baffle-to-tank-wall intersections then also become communication paths to bring liquid to the tank outlet.

If the mission requirements include known high accelerations which tend to displace propellant from the outlet, followed by a low-g period prior to propellant withdrawal, a small outlet retention screen can be used in conjunction with a total communication device as shown in Fig. 5. Because of its small size, the outlet screen will withstand the high adverse acceleration and keep the outlet filled, and a total communication device like the cross concept will draw propellant back into communication with the outlet screen after the disturbance passes.

Capillary System Flight Experience

Surface tension/capillary systems have been flown on spacecraft and upper stages such as Agena, Apollo and Transtage as well as on drone aircraft such as MQM-74A (Northrop) and Firebee II (Ryan). Flight service of smaller capillary propellant management feed systems has been demonstrated on spacecraft by Electro Optical Systems auxiliary ion propulsion systems on the Applied Technology Satellites (ATS) IV and V. These systems are listed in Table 2.

Table 2 Summary of flight experience

Flight application	Basic function	Number of flights
Current Agena	Propellant retention and propellant supply during low-g restarts	>120
Apollo Service Module	Propellant retention and gas phase flow blockage during propellant settling	11
Apollo Lunar Excursion Module	Propellant retention in feed line	6
Transtage	Gas phase flow blockage during propellant settling	20
ATS Cesium Ion Propulsion Subsystem	Vapor phase propellant feed	3
MQM-74A Drone	Gas phase flow blockage	322
Firebee II Drone	Gas phase flow blockage	9

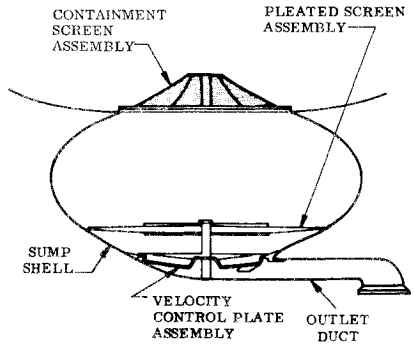

Fig. 7 Agena oxidizer sump assembly.

Current Agena System Requirements

This discussion covers the current Agena propellant management system only; a system for Improved Agena, discussed later, has not yet been implemented in flight. The system now in use (Fig. 6) was initially flown in 1964. More than 120 flights have been made with this system, which eliminated the requirement for ullage rockets and improved payload capability by reducing the amount of residual propellants. Since it was incorported as an engineering improvement on an operational vehicle, its design was constrained by the geometry and propulsion system requirements listed in Table 3. Each propellant tank is equipped with a sump. The oxidizer sump assembly is depicted in Fig. 7; the fuel sump is similar. Each consists of a very oblate spheroidal cavity capped with a containment screen shaped as a cone frustum which extends upward into the bottom of the propellant tank. The volumes contained between the screens and the propellant isolation valves (see Fig. 6) are 0.67 ft^3 and 0.51 ft^3, corresponding to 65.5 lb of contained oxidizer and 25.0 lb of contained fuel, respectively. These amounts are sufficient to supply the engine during low-g engine start and reorientation of the bulk propellant to the tank bottoms. After reorientation, the propellants refill the sumps, maintaining the engine propellant supply until engine shutdown or propellant depletion. The pleated screen assemblies (Fig. 7) prevent the liquid/gas interface (surface dip) from penetrating the sump outlet during low-g restart and act as gas barriers during sump refill. In the oxidizer sump, a velocity control plate assembly reduces the peak propellant velocity of the flow turning the corner into the sump outlet duct, delaying depression (high-g surface dip) of the liquid/gas interface into the outlet during propellant depletion.

Most Agena vehicles fly in a nose forward attitude, so atmospheric drag tends to deorient propellant away from the tank outlets. Because of main engine thrust tailoff and the thrust produced by a propellant vent system (to evacuate engine feed lines), there is a settling acceleration that nominally exceeds drag deceleration for about 30 to 40 min after engine shutdown, and no bulk propellant motion occurs. If the coast period between first and second burn exceeds 90 min, the drag force becomes dominant even for $+3\ \sigma$ venting thrust conditions, regardless of orbit altitudes, and the Agena definitely relies on the containment screens. If a screen were to fail to work, the next engine operation would occur with severe gas ingestion, even if propellant were repositioned at the outlets prior to engine ignition (the sump cannot refill unless a relatively high settling acceleration is provided). Ground tests, which intentionally introduced pressurization gas into the engine, have shown the transient characteristics

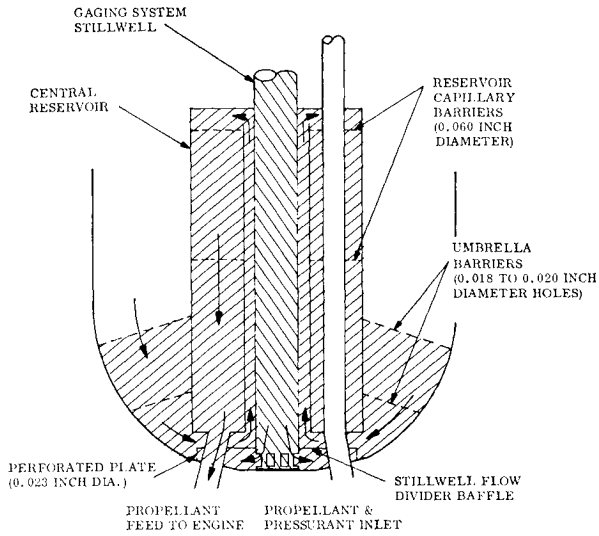

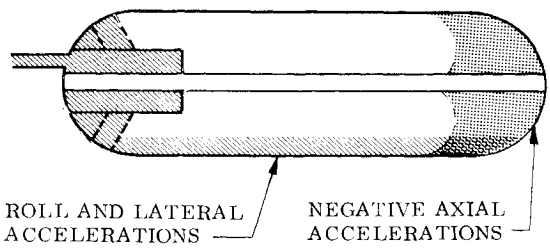

Fig. 8 Apollo SPS propellant acquisition system and retention modes

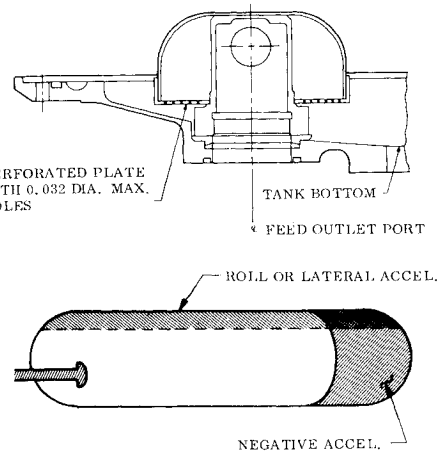

Fig. 9 LEM propellant retention system and retention modes.

to be expected from the turbine speed, chamber pressure, and pump inlet pressure if gas ingestion occurs. Of 27 Agenas that have flown with coast periods long enough to assure deoriented propellants, 22 experienced vehicle maneuvers just prior to engine restart which settled propellant over the outlets, and 5 restarted with deoriented propellants (as confirmed by accelerometer records). In all cases restart was successful and subsequent chamber pressure behavior was normal with no apparent gas ingestion.

The gas arrester screen and velocity control plate are also designed to allow maximum tank draining. The Agena depletion point values used for mission planning were derived from 1-g bench testing and have been confirmed by flight checks using two techniques. One consists of noting the behavior of the pump inlet pressure-time histories. As the propellant level drops in the tank, the change in hydrostatic pressure per second at the pump inlet becomes more rapid due to the head-volume characteristics of the spherical tank bottom; the changes follow definable trends that allow liquid level at any time to be relatively well defined. The second technique, which is more accurate, takes advantage of the operating characteristics of the propellant dump system, which dumps all residual propellant overboard after final engine burn. Tank pressures remain constant during the initial liquid phase dumping and then decay when propellant vapor and pressurization gas dumping begins. Since liquid dump flowrates are predictable, the duration of the constant tank pressure period after dump valve actuation defines the mass of liquid dumped, which is subtracted from the liquid onboard at shutdown to define residuals within ±2 lb.

Apollo SPS System Requirements

The Apollo Service Propulsion System (SPS, Fig. 8) is required to perform multiple engine firings following essentially 0-g coast periods, which may have been interrupted by adverse vehicle accelerations caused by the reaction control subsystem (RCS) and docking maneuvers with the Lunar Excursion Module (LEM). To ensure liquid feed to the engine during the start sequence, propellant settling thrust from the RCS is used in conjunction with a capillary propellant retention reservoir to minimize the amount of RCS propellant required. The initial configuration of the retention system consisted of the central reservoir only. The reservoir was designed to retain 4 ft^3 of propellant at the engine inlet at all times. The reservoir contains two capillary barriers, each consisting of a 0.060-in.-diam perforated sheet sandwiched between two layers of $\frac{1}{8}$-in.-cell honeycomb, to prevent displacement of propellant within the reservoir by pressurant gas during low-gravity lateral accelerations. In addition, the screens prevent large bubbles that may be entrained in the liquid from entering the feed line. The lateral screens trap the bubbles. As the gas accumulation increases to the point where the liquid flow pressure drop across the barrier exceeds the bubble restraining pressure, the gas is forced through the screen in the form of small bubbles which can be satisfactorily digested by the engine.[3]

Subsequently the performance was improved by adding two umbrella screens (perforated plates) nested into the lower dome of the tank to prevent displacement of propellant pressurant gas at the reservoir inlet during 0-g coast and to prevent foamed propellant from entering the reservoir during SPS burn following RCS propellant settling. As liquid descends to the bottom of the tank, there is considerable turbulence and intermixing with the pressurant gas. The umbrella

Table 3 Agena propellant management system constraints and requirements

Propulsion system thrust	16,000 lb
Minimum impulse bit	30,000 lb-sec
Number of restarts	one (multiple demonstrated in flight)
Propellants	UDMH/IRFNA
Maximum allowable reorientation gas ingestion	Negligible
Maximum steady adverse acceleration	
Longitudinal	$1.2 \times 10^{-2}\ g_0$
Lateral	$5.0 \times 10^{-3}\ g_0$
Minimum expulsion efficiency	99.9%
Maximum flowrate during low-g	48 lb/sec (oxidizer)
Preflow conditions	18 lb/sec (fuel)
Maximum steady flowrates	40 lb/sec (oxidizer)
	15 lb/sec (fuel)
Geometric constraints	60-in.-diam tanks, hemispherical ends, offset pump inlet locations

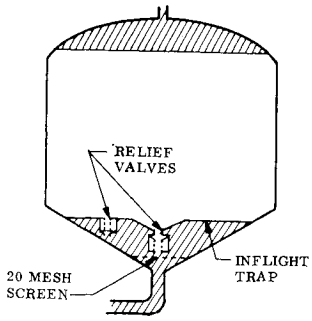

Fig. 10 Transtage propellant acquisition system.

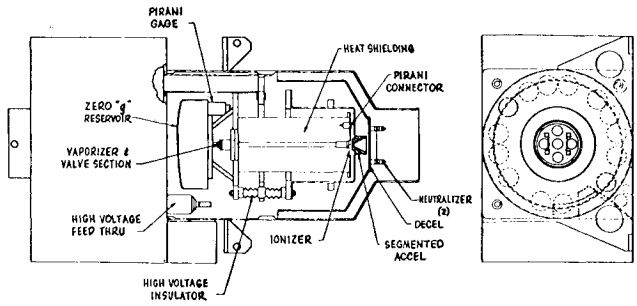

Fig. 11 Ion propulsion system schematic.

screens maintain relatively clear propellant beneath them with nearly all of the foaming restricted to the partially settled propellant above the upper screen.

The flow divider baffle at the base of the stillwell was added to increase the lateral acceleration level at which draining of liquid from below the umbrella barriers would occur when the tank was less than half full. Under these conditions, the propellant in the stillwell will drain out, providing a potential path for the pressurant to enter below the umbrella screens. This gas flow will be arrested by the 0.023-in. hole size screen around the periphery of the flow divider baffle. Additional improvements that have been suggested, but not incorporated to date, include antisiphon holes in the stillwell and additional retention screens.

As of April 1970, 11 Apollo SPS flights had taken place. The first two contained only the central reservoir, but the umbrella barriers were included on the others. Except for the first suborbital flight, which revealed an inadequate structural design, no difficulties were encountered. Operation was satisfactory on all flights. Several engine restarts were accomplished following various maneuvers and coast periods. Sufficient telemetry monitoring is performed to detect any significant gas ingestion in the engine feed line. Indication of the specific tankage malfunction could be obtained from the feed line interface pressure or the injector inlet pressure associated with that propellant while the engine chamber pressure and the vehicle integrating accelerometer (ΔV) would detect the presence of gas phase flow in either propellant. Ground testing has demonstrated the capability to detect mixed phase flow with the pressure measurements and established their characteristic behavior for this condition. The sensitivity of the ΔV measurement is sufficient that it would also detect any appreciable change in the engine thrust level as would be associated with gas ingestion in the feed system. Based upon the flight data (Table 4), the propellant management system performed in a satisfactory manner.

Lunar Excursion Module

Although the LEM tankage does not use a capillary propellant management system as such, an inverted metal can with a perforated barrier over the open end (Fig. 9) is used. The design is essentially the same for both propellant tanks and both descent and ascent stages. The inverted can retains propellant under negative accelerations, whereas the perforated plate prevents drainage due to lateral accelerations. Bulk propellant settling is accomplished prior to low-g main engine restarts with the ACS thrusters. Although it is difficult to determine whether propellant migration away from the tank outlets occurred on any of the flights, satisfactory engine operation was achieved on all flights.

Table 4 Numbers of Apollo systems flights through April 1970

SPS missions	Flights	LEM missions	Flights
Sub orbital unmanned	4[a]	Unmanned Earth orbital	1
Earth orbital	2	Manned Earth orbital	1
Lunar orbital	5[b]	Lunar landing	2
Total	11	Lunar orbit	1
		Circumlunar (aborted lunar landing mission)	1
		Total	6

[a] First two flights did not use umbrella barriers.
[b] Last flight was aborted with only single SPS mid-course burn.

Transtage

The Transtage employs a capillary screen barrier at each tank outlet (Fig. 10) to prevent large entrained gas bubbles from entering the feed duct. It is operationally the same for the fuel (A-50) and oxidizer (N_2O_4) tanks. The tanks contain false bottoms with check valves to prevent propellant migration away from their outlets. Prior to main engine restart, a propellant settling maneuver is accomplished with the ACS engines. Any gas bubbles larger than 0.035-in.-diam that were entrained as a result of the propellant reorientation would subsequently be blocked from passage into the main engine feed line by the screen. Although the need for this barrier has not been established in flight, the Transtage has performed many low-g restarts with up to three engine burns per flight without detectable premature gas ingestion by the engine system.

Cesium Contact Ion Spacecraft Auxiliary

Five cesium contact ion propulsion systems employing surface tension propellant feed have been flown. These microthrust systems (Fig. 11) were designed to provide a portion of the stationkeeping requirements (east-west disturbance induced by the triaxial Earth) of geosynchronous spacecraft. The thruster is a single-aperture contact ion engine with a segmented accelerating electrode for thrust vectoring and redundant thermionic electron emitters for ion beam neutralization. Cesium propellant is supplied to the thruster by a surface tension zero-g feed system with a thermally actuated valve. Thrust is adjustable in 5-μ lb steps between 0 and 20 μ lb by adjustment of power to the vaporizer.

The propellant feed system is a modified version of systems previously developed by Electro-Optical Systems.[8,9] Surface tension forces establish and maintain stable liquid-vapor interfaces and transport the liquid from the reservoir to the vaporizing area. The propellant storage reservoir, shown disassembled in Fig. 12, consists of a cylindrical volume enclosing a fin array. The gap between fins tapers from the outside toward the central axis of the reservoir. There are 120 fins with a spacing of 0.064 in. between fins at the outside edge of the array. Liquid Cs in the area between fins is forced toward the central axis of the reservoir and into contact with a porous nickel rod which carries it to the vaporizing surface.

The capacity of the unit is 50 g of cesium, sufficient for a 2-yr mission at 60% duty cycle. The porous rod is 40%

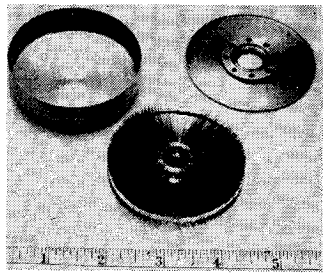

Fig. 12 Ion system propellant storage reservoir.

dense foam nickel approximately 2 in. long by $\frac{1}{8}$ in. in diameter. It extends from the rear of the reservoir through the mounting flanges and up the thruster feed tube to the vaporizer heater section. The feed system operates in a closed-loop mode; i.e., deviations from the required beam current cause more or less power to be delivered to the vaporizer. The vaporizer is able to cool rapidly by heat conduction to the reservoir and is heated rapidly by the vaporizer heater. Thus, rapid response times can be achieved both in turning on and in turning off the system. Prior to flight, operation of the feed system was demonstrated by laboratory, 0-g drop tower, and C-131 aircraft testing.

Of the three flight systems (five cesium engines) flown to date, orbital testing of only two engines has been possible. No data were obtained from two of the flights because of other vehicle malfunctions. The successful testing of the two ion engines was onboard the Applications Technology Satellite, ATS-IV.[10] During ion engine tests, numerous thrust level commands were sent to the engines. Telemetry data indicated satisfactory feed system response and operation.

Target Drone Applications

Another application of capillary propellant management systems is on turbojet-powered target drones.[5,11] Although the basic requirements are considerably different than most spacecraft systems, the same design considerations and basic capillary theory apply. The drones typically utilize JP-4 or -5 as a fuel and are ground-launched with a single continuous engine burn. During powered flight they may perform flight maneuvers that preclude conventional gravity orientation of the fuel at the tank outlet. Previous fuel withdrawal techniques utilized various combinations of accumulators, flapper valves, check valves, or other mechanical devices. Currently, two drones, the Northrop MQM-74A and the Ryan Firebee II, use capillary systems. Subsequent discussion is restricted to the MQM-74A (Fig. 13), but operation and design concepts are essentially the same for both systems.

During operation, the capillary elements act like gas-phase check valves as long as at least one of them is in contact with the fuel. Elements are located in the fore and aft ends of the fuel tank to ensure liquid contact during climbs and dives. Inverted metal cups or hoods over the elements form fuel reservoirs around the elements during negative-g maneuvers. Each hood contains a small hole in the top for venting during tank filling. The capillary elements are constructed of stainless steel wire cloth in the 10-μ effective pore size range. Pleated material is used to increase the flow area to obtain a low-pressure-drop design. The retention capability of the wetted material is sufficient to prevent vapor break-through under the operational acceleration environment. Figure 13 illustrates the system operation under two different accelerations. It is of interest to note that surface tension forces also tend to prevent water (which may have been introduced into the tank as a contaminant) from entering the fuel system in the submerged portion.

As of March 13, 1970, 322 launches of the Northrop MQM-74A were conducted on 159 different vehicles for a total flight time of approximately 121 hr, and 9 flights had been conducted with the Ryan Firebee II, with no apparent problems encountered in the expulsion system operation.

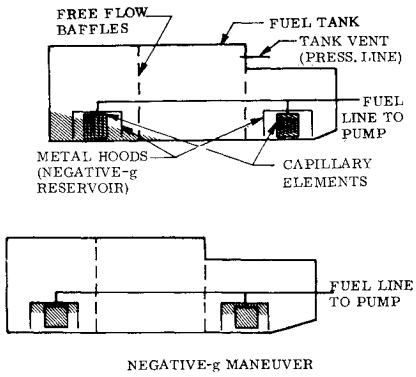

Fig. 13 Flight propellant orientation modes.

Although the operational target systems do not have telemetry to detect malfunctions, during the early part of the MQM-74A program the fuel system was monitored by telemetry. The data consisted of fuel flow and fuel pressure, which are both quite sensitive to mixed phase flow. Northrop reported that no interruption of fuel flow was detected prior to fuel depletion.

Propellant Expulsion System Analysis

Bulk Liquid Static Behavior

The propellant surface shape under low-g orbital conditions can be predicted accurately by available analytical techniques. Liquid in a container will seek a location and shape which produces the minimum total potential energy for the volume of liquid. The differential equation and boundary conditions describing the liquid surface under these conditions have been derived.[12] The resulting differential equation is nonlinear and cannot be transformed into an equation with a closed-form solution; numerical integration must be applied.

Digital computer solutions have been developed for several propellant tank geometries and a range of acceleration levels.[13,14] Elliptical approximations to several simple geometries have also been derived.[15] Graphical solutions to surface shapes, including relatively complex tank geometries, have also been successfully employed using Kelvin's technique.[16] Since any desired accuracy may be obtained, depending on the computation time expended, graphical solutions are particularly useful during comparison of expulsion system design alternates. When a design is frozen, graphical techniques may be applied more accurately, or a digital computer program can be written to cover the specific geometry of interest.

In tanks containing the total communication type of expulsion system, the concept of stability is not of interest and the fluid reaches its minimum potential energy condition regardless of the previous acceleration history of the tank, but for tanks which contain only partial retention devices, the concept of *stability* must be introduced. For these cases liquid will tend to remain in a given location in the tank, in spite of a deorienting acceleration, until a critical level of acceleration is reached; this level is referred to as the "stability limit" and is characterized by the dimensionless Bond number. For spherical tanks, there is no actual stability limit, and the liquid moves freely in response to any applied acceleration. For other tank geometries, the liquid tends to remain at one end until a finite stability limit is reached and then settles in the direction of the applied acceleration. The stability limit for these tanks is a function of both the contact angle (which is near zero for the most propellants) and the direction of the applied acceleration. Stability limit results have been derived for most tank geometries likely to be employed.[14,17–19]

Bulk Liquid Dynamic Behavior

When an acceleration in excess of the stability limit is applied to a tank that does not contain internal devices, the propellant settles to the opposite end of the tank in a mode which depends on the initial liquid surface shape. For the normal low-g spacecraft condition when the initial liquid surface shape is highly curved prior to the application of acceleration, the wall-bound reorientation process can be satisfactorily described analytically,[20,21] and the geysering which frequently results from this type of reorientation can be predicted. However, details such as reorientation sheet leading edge thickness, leading edge settling time, and pressurization gas entrainment have only been treated approximately; empirical definition of these quantities is required if accurate information is needed. Through conservation of dimensionless parameters, the test results derived by various researchers[1,22,23] can be applied to predict many new conditions of interest.

The sudden withdrawal of liquid from a container during low-g conditions forms a depression in the bulk liquid surface that may penetrate the tank outlet in some cases. Analytical techniques to describe this *startup surface dip* adequately have not been developed, and simulation testing is required to produce useful data on the behavior of a given tank design. The geometric complexity of many tank outlets contributes to the problem and may limit the usefulness of analytical effort in this area. This area represents one of the major gaps in the analysis of capillary system performance.

For situations where a *drainage surface dip* develops in an established flow situation, such as occurs at the time of propellant depletion, existing prediction methods and numerical results can be employed prior to development testing of a particular design.[22,24,25] Test results are available for comparison with the analytical predictions.[1,26,27]

Table 5 Example of propellant management system analysis[7]

Event	Description
1	Pad hold—gassing, condensation, gumming, etc.
2	Boost—entrapped gas clearing, condensate seal-off clearing, slosh wetting
3	Coast—capillary fill, bulk propellant orientation, etc.; seal-off due to slosh carry-over
4	Maneuver—short duration accelerations, slosh
5	Propellant transfer—steady primary mode and backup mode expulsion
6	Thruster start—transient feed from various propellant locations by primary and backup modes
7	Thruster burn—by primary, backup, and combined modes
8	Thruster shutdown—reorientation slosh carry-over after shutdown, heat soak
9	Propellant depletion—slosh, surface dip, propellant hang-up due to flow restriction and capillary effects
Phenomena involved in event	Events
Capillary retention	3–8
Pressure loss	5–7
Filtration	5,7
Structural integrity	2
Gas entrapment in outlet and clearing of same	2,5–7
Compression of entrapped gas	5–7
Gallery hole capillary "seal-off"	1,2,8,9
Seal break	1–3,7,8
Forward gallery capillary fill (gas ejection)	3–7
Gallery bubble growth and bubble travel	3–7
Gallery bubble shrinkage	3
Gallery/tank-wall fillet feed	3–7
Flow and capillary change due to hole stoppage	6–9
Heat soak-back	3,8
Outlet gas arresting	3–9
Propellant entrapment	9
Requirements affecting performance of event	
Propellant quantity	3–8
Propellant flowrate	5–7
Propellant temperature	3
Body acceleration and sequence of events	All 9
Thrust alignment	6–9
Propellant storage	3–7
Flight pressurant:	3–7
Tank preparation (e.g., cleaning and passivation)	3–9
Pad life:	1,3–7
Orbit life:	3–7
Design elements involved in event	
Fill and drain system	1,2
Pressurization system	1
Capillary fill vent screen	1–3
Gallery windows	All 9
Gallery wall surface finish	1–3,7
Gallery cross section area	3,5–9
Gallery/tank spatial relationship	1,3–9
Gas arrester/filter arrangement	All 9
Gallery base support structure	2–5
Gallery cross-sectional form	2–7

Empirical Inputs for Design

The capillary retention capability of a screen or perforated material can be predicted from a knowledge of hole geometry and kinematic surface tension,[17] but this prediction will usually be somewhat optimistic. For this reason, the ratio of actual to theoretical retention capability (ϕ) must be tested with the propellant and screen/perforated material of interest, using a test apparatus such as described in the following section. Similarly, for retention in other expulsion system devices, such as the corners of intersecting baffles or parallel plates, theoretical retention capabilities may be derived, but

Table 6 Performance testing summary[a]

Mission event	Dominant variables[b]	Dominant numbers[c]	Scale ratio (L_m/L_p)
Capillary fill[e,g]			
Gallery and gallery standoff fillet	g,σ,I,μ	We,Re,Fr^d	$\frac{1}{20}$[i]
Capillary retention			
Bubble sensitivity to evaporation	g,σ,e	Bo	$\frac{1}{1}$
Steady flight acceleration	g,σ	Bo	$\frac{1}{5}$
During primary (gallery) mode withdrawal	σ,g,v	Bo,We,Re	$\frac{1}{5}$
During backup (fillet) mode withdrawal	g,σ,v	Bo,We,Re	$\frac{1}{103}$
Shock	σ,I,g	Bo,We^i	$\frac{1}{5}$
Low-g propellant withdrawal			
Thruster operation	g,I,σ	Fr,We^d	$\frac{1}{5}$
Propellant transfer	g,I,σ	Fr,We	$\frac{1}{103}$
Backup fillet mode	g,σ,I	Fr,We	$\frac{1}{103}$
Expulsion efficiency[g]			
Thruster firing	g,σ,I	Fr,We	$\frac{1}{5}$
Propellant transfer	g,σ,I,v	Fr,We,Re	$\frac{1}{103}$
Propellant reorientation			
Gas ingestion	I,g,σ	$Fr,We^{f,h}$	$\frac{1}{5}$

[a] All are 1-g bench tests, except first, which is low-g drop test; all are with water as test fluid, but second also is IPA.
[b] g = acceleration; α = surface tension; I = inertia; μ = viscous force; v = velocity effects; and e = evaporation.
[c] The dimensionless numbers (Bo = Bond, Fr = Froude, Re = Reynolds, Ri = Richardson) and discussions on similarity testing are given in Refs. 1, 13, and 17.
[d] Since $Bo = We/Fr$, satisfying both the Fr and We numbers also satisfies the Bo number.
[e] For transient processes, such as propellant flow buildup and decay during thrust valve opening and closing, time scaling is also required.
[f] Simulation of screen gas barriers requires conservation of We.
[g] Quantitative prototype results, such as gallery fill times and residual propellant, must be obtained by appropriate scaling of model test results.
[h] Simulation of prototype gas bubble buoyant/inertia effects requires conservation of $Ri = gL(\rho_L - \rho_g)/V^2\rho_L$. (For normal test fluids $\rho_{liquids} \gg \rho_{gas}$ and Ri can be replaced by Fr^{-1}).
[i] Scale ratio chosen for suitability with facility test equipment.
[j] Analyses and tests have shown that the major system impact is arresting of the fluid disturbance.

the limited test results to date show that empirical correction factors again will be needed.

System designs often include screen elements to delay or prevent the entrance of gas into a tank outlet during startup or drainage surface dipping (or during a slosh which partially uncovers the outlet. Analytical methods have been useful in approximate screen sizing,[17] particularly where severe surface dip conditions are not experienced. However, the transient nature of the dip to be arrested and the complex geometry typically encountered in expulsion devices do not permit accurate analytical description of more violent surface dip behavior characteristic of multistart pump-fed propulsion systems, and therefore simulation testing must be employed.[1,28]

Performance Testing

Model testing based on similarity principles has been used for years to predict the prototype performance of aircraft, missiles, ships, water flow, etc.[29,30] The fundamental principle of similarity testing is that conservation of the governing dimensionless groups will yield identical scaled behavior of the model and prototype. To assure that a spacecraft propellant management system design satisfies all mission requirements, the prototype operational sequence must be defined, and similarity tests conducted conserving the model and prototype dimensionless groups by proper specification of the model size, acceleration, flowrate, and other environmental test conditions to assure that fluid behavior in each model represents the scaled performance of the propellant in each respective prototype operational sequence being evaluated. Simulation techniques and subscale test equipment[1,31–35] have provided extensive data demonstrating the accuracy of scaling results. These techniques are currently employed to verify analytical predictions and to obtain data where analytical methods are not practical.

For example, the propellant management system for a 62-in.-diam, spherical hydrazine tank[7] was not designed for capillary propellent retention in a 1-g acceleration field, since this would require prototype screen holes of about 0.00003-in. diameter. To assure that the chosen design would meet the mission requirements, the complete operational sequence was formulated (Table 5), and the propellant management system performance was shown to satisfy all requirements by a combination of analyses and tests. Each function in Table 5 was analyzed or tested to assure compliance with the mission requirements. The choice of analysis or test was based on two elements: 1) confidence in analysis techniques and 2) the degree of mission operational complexity and applicability of previous test data to this particular system. The events selected for evaluation by similarity testing are summarized in Table 6. They were analyzed to determine the dominant forces controlling each event and were then evaluated to determine the best test method. Following this, the dominant dimensionless groups were determined and used to calculate the model scale and test conditions. Results of these analyses are also summarized in Table 6.

In many cases, the test method, test fluid, and scale ratio are not unique. One or more parameters may be selected and the others follow. In general, 1-g bench tests are simpler, less time consuming, and cheaper if the calculated model sizes are reasonable. Consider capillary fill of the gallery as shown in the first mission event of Table 6. The scale ratio is identified as $\frac{1}{2}_0$ for drop tower (0.01 g_o) testing with water as the test fluid. For a 1-g bench test, the scale ratio would become about $\frac{1}{2}_0_0$. The whole 62-in.-diam prototype tank would be reduced to about 0.3-in. for the model, which is unacceptable considering boundary-layer effects and test visibility. Since the drop-tower capsule acceleration is variable, it is set by specifying water as the test fluid and choosing a scale ratio large enough to eliminate boundary effects and provide good model visibility. Similarly, specifying a test fluid with half the kinematic surface tension of water would require a reduction of the model scale to about $\frac{1}{3}_0$ or, alternatively, a reduction in the model acceleration by a factor of 2. Although similarity testing allows great freedom in choosing at least one of the test variables, caution must be exercised in setting the scale ratio when quantitative results are required. For depletion point testing, small scale ratios can result in significant errors since small model volumetric biases are magnified by the cube of the scale ratio.

Test Methods

The best technique is the one which closely simulates the prototype environment and is simple, reliable, convenient, and inexpensive. Generally, no one technique satisfies all these requirements, but 1-g bench testing in one or more forms comes closest. In cases where the prototype acceleration is within two orders of magnitude of 1g, withdrawal and static and dynamic propellant behavior may be readily simulated through model sizing and test fluid substitution. This type of bench testing is applicable to transient and steady-state propellant withdrawal evaluation and to testing of propellant static retention and bulk settling once the settling mode and downflow rates have been determined.[1,12,13,17,27,35–38] For very low prototype acceleration environments, techniques for reducing the propellant body forces must be applied. In some cases, a good simulation is obtained in 1g by using immiscible test fluids with near identical densities. In this manner, the low buoyancy of the substitute propellant simulates the low-g body forces on the prototype propellant.[12,13,3]

Table 7 Similarity test approach comparison

Type	Approach	Application	Strengths	Limitations
1-g bench	Use dimensionless groups to scale model size, test fluid properties, and test conditions	Evaluate propellant withdrawal, bulk static and dynamic behavior	Convenience; controlled test conditions; rapid turnaround and low cost	Model size becomes small at low prototype accelerations; does not duplicate low-g initial conditions
Immiscible test fluids	Immiscible test fluids with similar densities reduce body forces	Evaluate bulk propellant configurations	Convenience; controlled test conditions; rapid turnaround and low cost	Limited to static bulk evaluations
Electro-magnetic field	Colloidal suspension of magnetic particles "supported" by electromagnetic field	Evaluate propellant withdrawal, bulk static and dynamic behavior	Variable body forces and precise control of test conditions	Model size limited by size of magnet; does not provide low-g simulation of gas or vapor phase
Aircraft testing	Keplerian trajectories used to produce weightlessness	Evaluate propellant withdrawal, bulk static and dynamic behavior	Produces true low-g environment for relatively long periods	Poor control of g magnitude and initial conditions; relatively expensive and time consuming
Drop tower	"Free fall" of test platform	Evaluate propellant withdrawl, bulk static and dynamic behavior	Precise control of test conditions; reasonable test turnaround; variable body forces	Relatively short test period; small models for modest facilities

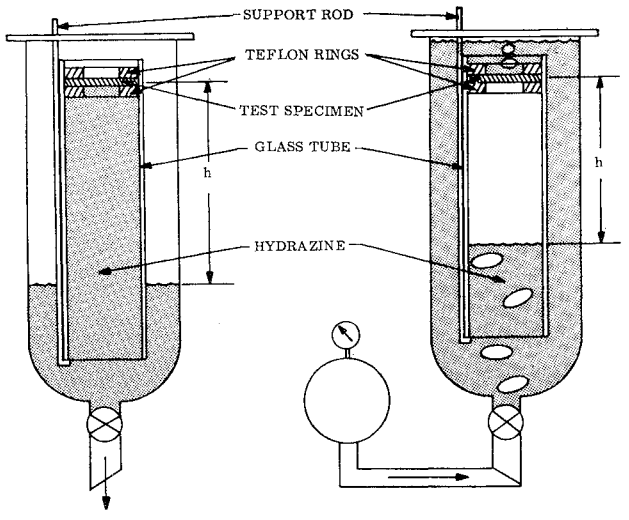

Fig. 14 Static and dynamic retention test apparatus.

Another technique recently developed uses a colloidal suspension of magnetic particles in the test fluid which is "supported" by an electromagnetic field. The field strength is adjusted to simulate the low-g body forces on the prototype propellant.[33,35,37]

Low-g aircraft testing techniques[12,13,17] based on Keplerian trajectories yield relatively long periods (~32 sec) of low-g environment at the expense of rather uncontrolled initial conditions and higher test cost. From the experimenter's point of view, drop-testing is the most satisfactory low-g technique and has received the most attention.[12,13,17,23,39-42] The experiment platform is enclosed in a drag shield, which absorbs the aerodynamic drag while the experiment platform free-falls or is accelerated to a prescribed acceleration by a constant-force spring or cold-gas thruster. Experiment times have been extended to 10 sec with "pop up" facilities, such as the one at NASA Lewis Research Center. Generally, a simple free-fall tower of ~100 ft with usable free-fall time of ~2.3 sec is sufficient to simulate the prototype event. The following paragraphs present typical propellant expulsion and bulk behavior data obtained from these tests, and Table 7 compares several test approaches.

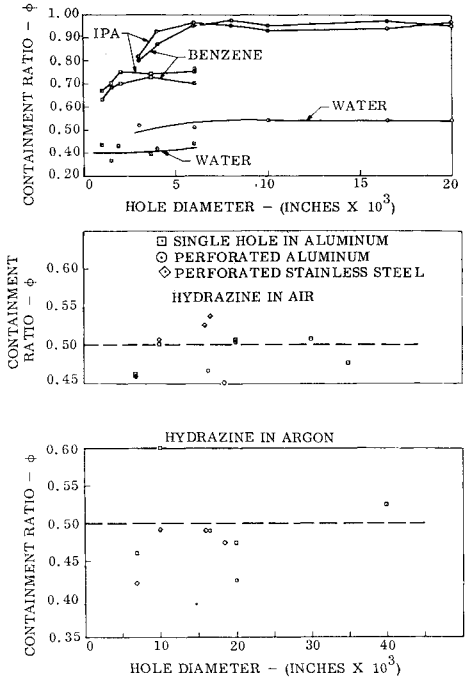

Fig. 15 Static retention test results.

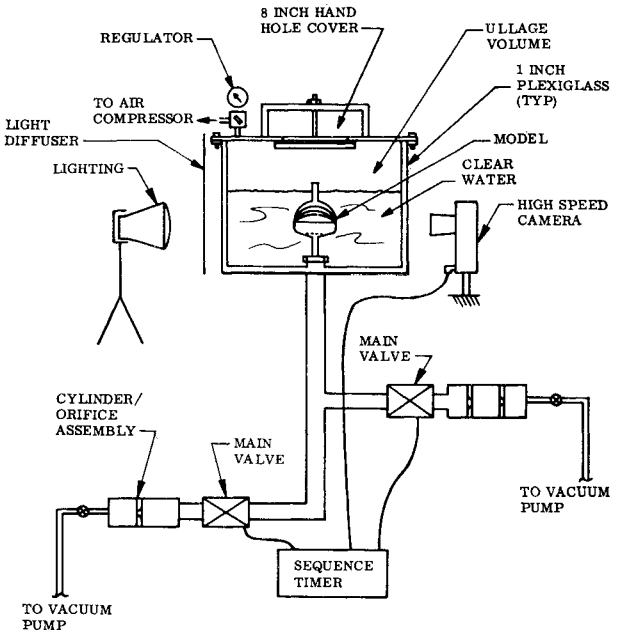

Fig. 16 Restart test apparatus.

Bench Testing at 1g

In some cases, high degrees of precision may be obtained by bench-testing; in others, approximations of complex phenomena may be obtained rapidly to enhance understanding and suggest approaches for analysis and design. For example, propellant retention with typical materials of construction can be determined with good precision. It depends on fluid surface tension and the contact angle of the fluid on the retention device at all points along the gas/liquid interface. Different fluids and materials of construction behave quite differently[13,43,44]; each combination must be tested in a manner simulating actual flight loading.

The preferred method of testing for static retention is shown in Fig. 14. The fluid is supported by individual meniscuses at the screen grid in a manner similar to the flight loadings. The fluid external to the tube is drained until the test grid will no longer support the head, and the breakdown point is recorded. Repeatability is determined for several "design" grid samples, then the grid is loaded to near demonstrated capability to assure longevity of the retention under simulated flight conditions of grid material, propellant, and gas

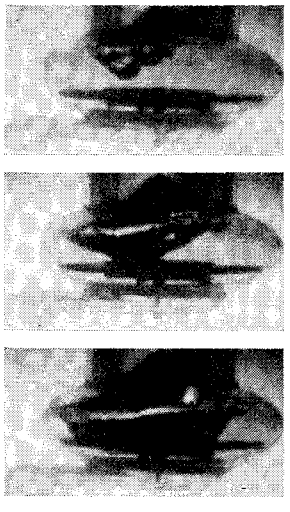

Fig. 17 Low-g surface dip development.

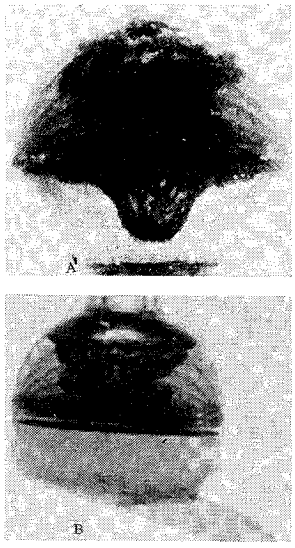

Fig. 18 Improved Agena surface dip.

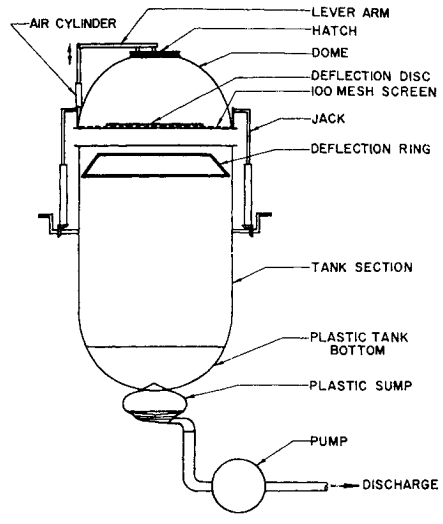

Fig. 19 Geysering and refill equipment.

(pressurant and propellant vapor). Data are recorded as percent of theoretical capability based on equivalent grid radius, propellant surface tension, and contact angle. Results for several fluids, grid constructions, and grid sizes are shown in Fig. 15. The range of results demonstrates the importance of this type of testing to expulsion system design.

Dynamic retention is usually associated with the hydrostatic expulsion of gas from a retention device as shown in Fig. 14. For hydrazine, the dynamic retention head capability was almost twice that of static retention, ($\phi \approx 1$), demonstrating the importance of accurate simulation of the flight grid loading. Use of static test results might predict much less gas trapped under the retention device than would be experienced in flight.

Transient propellant withdrawal is another key problem faced by the expulsion system designer.[26,27,36,45–48] The problem is magnified for multistart spacecraft equipped with pump-fed propulsion systems where significant quantities of one or both propellants are withdrawn from the propellant tanks before thrust chamber ignition. For a unidirectional thrust multistart system, it is common to equip each tank with a small sump at the outlet to supply propellant to the thruster until vehicle acceleration settles the propellant to the tank bottom and refills the sump. A combination of sump geometry shaping and screen placement is employed to prevent the liquid/gas interface from being depressed into the tank outlet. The geometry shapes the propellant velocity profile while the capillary forces arrest depression of the interface. Nonaxisymmetric sump geometries do not lend themselves to accurate analyses, and design concept performance must be verified empirically. An example of specialized bench testing equipment is shown in Fig. 16. It utilizes a closed plexiglass box to pressurize the sump model and valves, and evacuate receivers equipped with orifice assemblies calibrated to control the profile. The valves have linear flow areas vs poppet travel, so that linear flowrate ramps may be obtained by regulating the valve opening times. After valve opening, the prescribed steady flowrate is provided by the calibrated orifices until the downstream volume is filled. By suitable arrangement of valves, orifices, and volumes, the desired combination of ramp or step changes in flowrate, steady flowrates, and flow durations are obtained to simulate the prototype flow transients. Over-all system calibration is conducted by substituting a graduated cylinder for the sump model. Test results are recorded with a high-speed camera.

An understanding of the basic phenomena, supported by analyses of the governing equations and boundary conditions, is required to determine the appropriate dimensionless scaling parameters. For the Agena and Improved Agena vehicles[1,2] and the Froude and Weber numbers were determined to be the appropriate scaling parameters (Table 8). Based on the prototype propellant properties, flow transients, and vehicle acceleration, the model scale as well as test fluid and flow transients were determined. Models were tested to simulate restart of the Agena pump-fed engine at about 0.02 g. The surface dip phenomenon was highly exaggerated relative to 1-g performance. The pictures in Fig. 17 illustrate the development of a low-g surface dip in a $\frac{1}{4}$-scale model of the oxidizer sump. The screen shown in Fig. 7 was pleated to provide a larger flow area and was developed through experimentation to suppress the liquid-surface dip. The mesh size of this screen was chosen so that surface tension forces exceed inertia forces ($W_e \ll 1$), and consequently, no gas penetration occurs; rather, as seen in Fig. 17, a flattening or spreading of the surface dip takes place over the screen. The picture sequence clearly indicates that the surface dip is dominated by the flow inertia. Tests conducted with an early design concept for the Improved Agena system showed that the surface

Table 8 Agena similarity testing comparison*

Agena type	Item	Mission events: Capillary propellant retention	Low-g engine restart[e]	Propellant reorientation dynamics	Sump refill: High-g	Sump refill: Low-g	Expulsion efficiency[g]: High-g	Expulsion efficiency[g]: Low-g
Improved	Dominant numbers[c]	Bo	Fr,We^d	Fr,Re	Bo,We^f,Ri^h	Fr,We^f,Ri^h	Fr,We^f,Re	Fr,We^f
	Test method	1-g	1-g	1-g	1-g	Drop tower	1-g	1-g
	Model scale	$\frac{1}{4}$	$\frac{1}{4}-\frac{1}{6}$	$1,\frac{1}{4}$	$1,\frac{1}{4}$	$\frac{1}{4}-\frac{1}{6}$	1	$\frac{1}{4}-\frac{1}{6}$
Operational	Dominant numbers[c]	Bo	Fr,We^d	Fr,Re	Bo,We^f,Ri^h	NA	Fr,We^f, Re	NA
	Test method	1-g	1-g	1-g	1-g	NA	1-g	NA
	Model scale	1	$\frac{1}{4}$	1	1	NA	1	NA

* Footnotes are the same as given for Table 6.

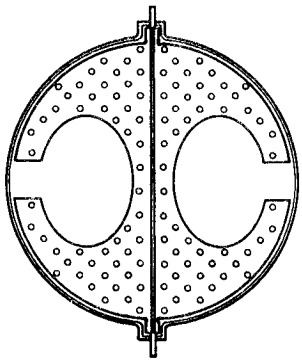

Fig. 20 ATS-F and -G design concept.

depression penetrated the gas arresting screen (Fig. 18a). The final design concept (Fig. 2) included increased capillary baffle freeflow (perforations), a velocity profile shaping plate below the gas arresting screen, and modified external sump geometry which eliminated the gas penetration as shown in Fig. 18b.

For a unidirectional thrust system, initiation of engine thrust will reorient the bulk propellant to the tank bottom. The geometry of the propellant downflow depends upon the propellant configuration prior to engine thrust, the vehicle acceleration, and the tank dimensions and internal geometry.[1,12,17,49–52] The prototype reorientation geometry and downflow rates must be determined by analysis and low-g testing. Once determined, the reorientation may be simulated with bench test equipment to provide data for evaluating the effect of reorientation on vehicle dynamics, to determine the capability of the sump design to prevent pressurization gas ingestion, and to evaluate the sump refill performance.

Figure 19 is a schematic of a representative reorientation test apparatus. The test fluid is allowed to accelerate under freefall to the desired velocity in a manner simulating the predetermined reorientation mode. The two important test components are the properly scaled tank bottom and the fluid reservoir; the latter is equipped with a quick opening hatch and a screen stretching across its bottom. On top of the screen is a deflection disk that shapes the reorienting flow during the test. The reservoir is filled and the test fluid retained within the reservoir by air pressure, since the liquid interface is stabilized within the properly sized screen mesh by surface tension forces. To initiate the test, the hatch is opened rapidly, producing a free surface above the test fluid. The initial downflow tends to drop straight to the tank bottom and must be deflected toward the wall by the deflection ring. In the prototype tank, there is only one free surface, and the liquid will follow the wall, as exemplified by the downflow in an inverted cylindrical container, if the free surface is not disturbed when reorientation is initiated. In the model, the liquid follows the wall once the flow accelerates because of the radial inertia of the liquid leaving the reservoir (vena contracta effect). The downflow thickness may be adjusted by proper sizing of the deflection disk within the reservoir. The propellant reorientation characteristics of the Apollo tank geometry were evaluated with bench test equipment.[40] Fluid viscosity, which affects the boundary-layer thickness during orientation, is unimportant for significant quantities of propellant, since the phenomenon is generally inertia-dominated. Therefore, by conserving the Fr to which the reorienting propellant is subjected, geysering can be readily investigated in a model. To evaluate the refill characteristics of a sump or stillwell, scaling of tank outflow rates and capillary devices must be accomplished to properly represent the prototype propellant behavior.

Low-g Testing

Although simple 1-g bench testing is preferred, in many cases, it may not be practical. Simulation of a low-g field usually requires a significant reduction in model size that at some point becomes too small, considering visibility, boundary layer effects, and acceptable model and measuring scale dimensional tolerance. For example, small model and scale dimensional errors may yield unacceptable accuracy limits when test results are scaled to prototype conditions. Also, some testing requires a low-g fluid interface geometry

Table 9 Factors obscuring material definition—example for metal

Process variables	Process	Material parameter affected
Residual impurities	Extraction from ore	Bulk composition
Furnace environment Alloying elements	Melt	Interstitial gases Bulk composition
Lubricants Total material pickup Work direction	Shaping	Surface macrostructure Grain size Grain orientation
Furnace environment Time and temperature Quench rate	Thermal treatment	Grain growth Interstitial gases
Filler amount Heat affected zone	Welding	Metallurgical distribution
Furnace environment Time and temperature Thermal gradients Quench rate	Thermal treatment	Grain growth Interstitial gases Metallurgical transformation Residual stresses
Process bath Composition	Pickling, passivation, cleaning	Surface macrostructure
Referee fluids Number cycles Stress rate	Testing	Fatigue
	etc.	

for initial conditions. One or more of these constraints necessitate reduction to zero gravity testing; a free-fall facility[12,13,17] is used for such testing.

Tests conducted in support of conceptual design studies for the version of the ATS-F and -G propellant acquisition system proposed by the General Electric Co. are illustrative of the use of low-g test techniques. The selected capillary device was a sheet metal right-angle cross along the central axis of a spherical tank (Fig. 20). It was predicted that the low-g propellant configuration would not be significantly perturbed by anticipated spacecraft lateral disturbances. In drop-tower tests, the model was allowed to free fall until the near zero-g propellant configuration was established, then a photocell beam was interrupted by the drag shield and initiated a cold-gas thruster to simulate the anticipated lateral disturbance, which, as predicted, did not perturb the propellant configuration. If the spacecraft disturbance had been produced by a reaction control thruster, propellant withdrawal could have been simulated by connecting the tank outlet to a valve and evacuated container. The valve could be actuated along with the cold-gas thruster; for accurate simulation, both valve and thruster poppets must be light and mounted in such a way that their actuation does not disturb the simulated propellant configuration. Simulation test techniques applied to the 62-in.-diam tank hydrazine and Improved Agena Propellant Management System and the ATS-F and -G hydrazine propulsion system design were based on the scale model performance test results. The model accelerations, propellant withdrawal rates, and timing were scaled by conserving the governing dimensionless parameters, determined by prototype event analysis. Test technique validity for these development applications was demonstrated by comparison of predicted and flight performance and by ground test cross-checks where the same dimensionless parameter values were obtained with models of different scale ratios.

Material Compatibility and Selection

Materials selected, including contained fluids as well as materials of construction, must be compatible with the total system environment. Among many factors encompassing total environment are those introduced during material processing (e.g., impurities) and during system fabrication (e.g., contaminants). Thus far, the large number of factors has stymied the development of a systematic means for selecting materials.

It has been common practice in other technologies to tolerate some amount of system deterioration due to incompatibility and to make provision for restoration through maintenance, repair, and replacement. This practice contributed to the lack of refinement of material selection technology to the level necessary for spacecraft. The use of more reactive propellants, longer mission durations, and vanishing weight margins aggravate the problem. The goal for material technology advancement may be stated as the ability to select materials which will cause less system deterioration than that which would result in the minimum acceptable level of performance at any point in the mission. The basic cause of incompatibility is thermodynamic instability—the tendency for materials collectively to reduce themselves to a lower energy state form. In the process they may lose desired attributes or generate new constituents detrimental to reliability. Knowing the interaction pathways accessible to the system, it should be possible to predict its state at any time if the state at time zero is known. However, even the determination of the interaction details by laboratory tests under isolated conditions using material test coupons is a major undertaking because of the numerous initial and resulting factors to be characterized and controlled. Predicting the progressions of the interactions in an expulsion system is, of course, even more difficult. Yet the study of interaction variables in their simplest terms is the approach which has contributed the most to a methodology of material selection. Any measures which would decrease the number and range of variables would lessen the breadth of the required methodology. Observe the numerous processes typically used in metal fabrication, for example, in Table 9. Each process is plagued by its own variables; one can appreciate the total variability possible in the end product. At present the processes are controlled to some degree by specifications such as the MIL Standards. The adequacy of such standards and quality controls need re-examination.

Much data has been accumulated for virtually all the materials and propellant combinations of interest,[53-57] so that it should be possible to select a system configuration free of gross incompatibilities, but specific tests may be needed; for example, to resolve stress corrosion and flow decay problems.[58,59] An additional obstacle to the development of a satisfactory methodology for long missions is the fact that there is no longer adequate time to characterize the time factor itself. A way must be found to compress the effects of the entire mission duration into a much shorter time span.

Some advantages of surface tension propellant acquisition devices, from the standpoint of material compatibility are 1) they can be constructed from virtually all metals, and choosing metals common to the rest of the system should eliminate galvanic couples and simplify joining procedures; and 2) they are passive devices and thus, not subject to cyclic stresses or plastic deformation which might result in stress corrosion or corrosion fatigue. The principal unknowns regarding their use are how well the interfacial forces (e.g., wettability), and the propellant's surface tension (σ) endure. From the relatively short missions flown to date, there is no evidence of deterioration of σ surface tension properties with age, but this possibility must be investigated. Decreasing with time has been reported for a class of liquids known as long-chain colloidal electrolytes.[60] Over a period of several days, σ was observed to decrease and eventually level out to $\sim 50\%$ of the initial value in the worst case. A comparable change in propellants could, in most cases, be compensated for by over-design. Tests in this area are in preparation at the Jet Propulsion Laboratory (JPL). The apparatus will provide a closed environment for a screen and propellant and a means of periodically measuring the bubble point of the screen. The bubble point can be equated to the capability of the propellant liquid/vapor interface at the screen to support a Δp, and it is a measure of both wetability and σ. Thus, except for changes in screen equivalent pore size—which would be determined after completion of the test, the test results will be relevant to all surface-tension device designs. The considerable material surface area afforded by the screen should serve to accelerate any incompatibility effects.

Other compatibility studies at JPL include a two-phase effort begun in 1962 for the Earth-storable propellants. In the first phase, 274 materials (elastomers, ceramics, and metals) and the propellants N_2O_4, N_2H_4, N_2H_4—$N_2H_5NO_3$ mix, and unsymmetrical dimethyl hydrazine (UDMH) were placed in sealed glass capsules, and the pressure rise was monitored using Bourdon tube gages, under controlled temperature conditions. The test coupons were partially immersed in the propellants. Some of the tests lasted 1500 days.[61,62] Phase II, which is underway, incorporates some basic refinements. The stainless steel Bourdon tube has been replaced with an external strain gage on the glass capsule, to eliminate any interaction between the gage material and the propellant/test coupon system. Automatic data acquisition and automatic data processing are being incorporated. The program will include dissimilar metals in contact, dissimilar metals not in contact, welded coupons, brazed coupons, plated coupons, and stressed coupons. A program goal is to maintain a high degree of control over-all phases of specimen preparation. Pre- and post-test analyses will determine changes in weight, color, and surface condition,

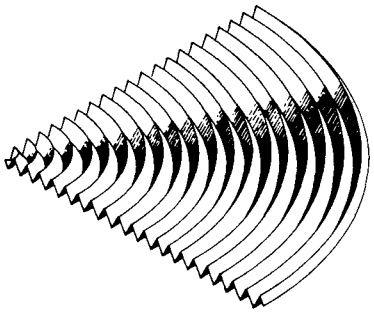

Fig. 21 Curved corrugation element.

and subtle effects, such as intergranular corrosion. Any decomposition products also will be analyzed. Materials for use with the space storable propellants OF_2, B_2H_6, and F_2 are being selected. The major portion of the program will expose typical materials to the propellants at −230°F. Effects of temperature, gas-liquid interface, welding, dissimilar materials, and stressed conditions will be simulated where practical. Other major current activities include studies on the formation and behavior of clogging materials in propellants, the effects of high levels of nuclear radiation upon the physiochemical properties of propellants and materials, and accelerated testing techniques.

Manufacturing

Propellant management systems flown to date have been made from commercially available materials and built in normal airframe manufacturing facilities. Special tooling has been of shop-aid variety. Designs now being considered, however, may create a need for greater use of clean rooms and less common manufacturing techniques such as electroforming, metal spraying, and electrical discharge machining. Much of the propellant management system manufacturing has involved square-weave stainless steel sintered joint meshes ranging from 85 × 85 to 400 × 400 wires/in. They have been developed into cones, pleated discs, plain discs, and other two- and three-dimensional shapes. The three-dimensional shapes have been generated by wrapping and folding techniques which preclude stretching and hole distortion.

Screen-to-screen attachments have normally employed direct resistance spotwelding through overlapped joints. Screen-to-sheet metal attachments have been done both by direct spotwelding and by sandwiching the screen between the sheet metal and a doubler and spotwelding the assembly. Stainless screen is being attached directly to aluminum sheet by resistance spotwelding. The heat and pressure introduced by the electrodes causes aluminum from the sheet to flow through the screen openings and, with the aid of the molten aluminum capillarity, around the wires so as to bond the mesh to the sheet. The bond gives the external appearance and the strength of a simple spotweld. All of the joints discussed are

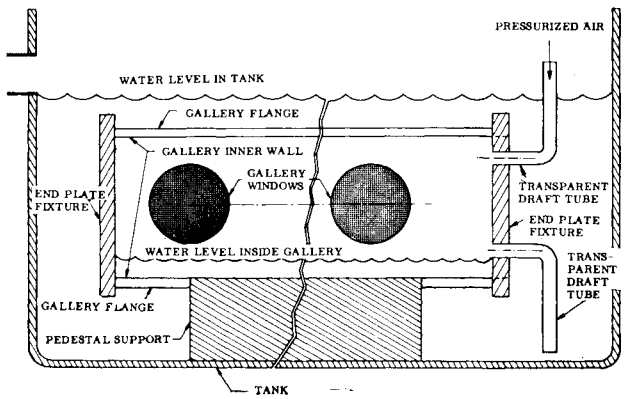

Fig. 22 Gallery assembly acceptance test.

structurally stronger than the adjacent wire mesh. Also, the spotwelding procedure results in minimal screen hole distortion, which causes no appreciable capillary degradation. Distortion occurs only in the immediate area of the spot where the small gap at that point between the locally distorted screen and the mating part produces a backup capillary as strong or stronger than that of an undistorted screen hole.

The need for minimal weight has led to thin wall constructions. One assembly now in production is nearly 5 ft in diameter and is constructed of 0.012-in. aluminum (Fig. 4). Flat areas of this assembly are beaded simply for the cosmetic purpose of preventing unsightly waving of those areas as the result of heat treatment. Another assembly, not so thin-walled but by necessity a submaximal efficiency pressure vessel form, is prestressed by internal pressurization prior to finish machining; this is done to prevent plastic deformation and associated excessive over-all dimensional growth in service. This prepressurization, which also serves as a proof pressurization, enables a considerable saving compared to what the vessel would weigh if its walls were simply thickened sufficiently to achieve the required structural rigidity in service.

One of the future designs may entail aluminum panels of less than 1 mil thickness (Fig. 21). These panels may be deeply and sharply corrugated, i.e., pleated over their entire dimensions, and for strength reasons, the pleat axes (fold lines) may be curved. When the manufacturing of these elements is undertaken, the decision must be made whether to develop such surfaces by first pleating along straight lines and then warping the pleat axes into the desired curves by successive mechanical dies—or by direct generation of the element through electroforming, metal spraying, high-energy forming, etc. Further, the decision must be made whether to form such parts from blanks preshaped to come out to the right final over-all dimensions after forming, or to trim to size after generation of the pleats by staking several elements together and grinding away excess material, or to trim by electric discharge machining, by chemical dip, by precision cutting torch, etc.

Assembly and Handling

Subassemblies consisting, in part at least, of screen elements are generally joined by mechanical fasteners or by welds of a kind which permit removal and replacement of a defective assembly. In the case of internal joints, the closeness of the connection usually need be only sufficient that the capillary capability of gaps at that point is equal to or greater than the capillary capability of screens used in the assembly. Until now, this has usually meant that gap widths in the connection could be permitted to be as much as one half (a factor depending on the ratio of the capillary capability of a one-dimensional opening, i.e., gap, to a two-dimensional opening, i.e., screen hole) the screen hole dimension.

Attachments of subassemblies to the total propellant management assembly and the tank shell must provide sufficient structural compliance to avoid excessive assembly stresses and high stress interactions due to pressurization. Further, the installation interface between the total assembly and the tank shell must permit access for tank cleaning and inspection of interior welds.

Future designs will incorporate such details as multilayered twilled screens. Such components will be very difficult to clean after assembly because of the contaminant catching nature of the twilled mesh and because of the relative inaccessibility of the middle layers of screen. The screen layers probably will be cleaned first and assembled under clean-room conditions, after which they must be protected from contamination. Certain elements of other future designs are expected to be structurally delicate in free-state form, even though not so in completed flight assemblies. These will require more careful assembly techniques than employed to date.

The handling of these systems to date has been little different than that of average aerospace flight equipment. When stored, some subassemblies are kept in heavy plastic envelopes and others in polyurethane boxes. Frequently the time space between cleaning and assembly is short enough that subassemblies are simply held in the clean room until installation. Certain shop-aid variety protective devices, such as sheet metal covers for screens and plastic bumper strips for thin sheet metal parts, are used during the fabrication process. Greater handling care will be required for certain future assemblies owing to probable use of very thin-walled parts and multilayered, fine mesh, twilled screens, as just discussed.

Acceptance Testing

Structural and performance acceptance tests are commonly performed on propellant management assemblies prior to their installation in tanks. A representative structural test is that of proof pressurization (which serves the dual purpose of a fabrication process pressurization as previously discussed).

Final verification of capillary performance capability of all systems produced to date is accomplished prior to installation. A rapid, economical, and accurate check on the capillary acceptability of both screen installations and relevant structural joints can be obtained by bubble testing. Defective locations can be visually pinpointed and identified for detailed inspection and subsequent disposition. Further, the procedure can give an accurate accounting for microscopic geometric peculiarities of individual holes that affect the ratio of actual to ideal capillary capabilities.

Many different setups are feasible for bubble testing a given component. The choices among candidates are made after consideration of test fluid availability, handling, and compatibility; initial special tooling cost; recurring labor cost; technician training requirements; clarity of test results; test background during development modelling; etc. The usual setup utilizes shop-aid variety special fixtures, water with corrosion inhibitor additives, and air normally available in clean rooms.

One example of a bubble test is that performed on a screen device designed to contain liquid within a housing under adverse accelerations. This test is performed simply by lowering the housing into the water tank, allowing the assembly to fill with water, capping the outlet of the housing, lifting the assembly (now full of water) from the tank, settling it on the shelf, and then observing the containment screen for water leakage (dripping). The criterion is zero dripping. This is a severe overtest relative to flight requirements and is performed to establish maximum confidence in the system. The representative setup of an assembly performance acceptance test of a propellant management system recently entering production is shown in Fig. 22a. The specific test item is half ($\sim$90° segment) of one of the gallery arms (loops) shown in Fig. 4. In this test, the ends of the assembly are capped with end-plate fixtures, after which the assembly is lowered into the tank shown and allowed to fill with water. Air is then introduced through the upper draft tube. Water is displaced from the assembly down to the inside level depicted, and gas bubbles from the lower end of the lower draft tube. The upper halves of the gallery windows (screen) shown and weld joints in the upper half of the assembly are observed for the escape of gas bubbles. The criterion is zero bubbling. In this setup, the screen holes and joints at the assembly centerline are tested at minimum acceptance levels. Screen holes and joints above this point are somewhat overtested—in accordance with the relative distance by which the point in question is above the lower end (outlet) of the lower draft tube. After the test is observed in this position, it is turned over, so that what was previously the lower half becomes the upper half in the next test. If again zero bubbling is observed, the part is performance accepted.

Summary and Conclusions

Adequate design concepts for capillary propellant expulsion systems have been developed to satisfy current and anticipated mission requirements. There is sufficient flight experience to verify performance on short-duration, storable-propellant missions. Performance analysis and simulation test techniques are adequately developed and proven. The long-life mission materials selection and compatibility problem is recognized, but adequate design data are available for short missions. Currently available fabrication and acceptance test methods are adequate for existing and anticipated design concepts.

The areas warranting further industry attention are: 1) development of accelerated materials compatibility evaluation including effects on design structural elements, the propellant chemical and capillary physical properties, and rates of gas evolution; and 2) the extension of Earth-storable capillary propellant expulsion system design technology to space-storable and cryogenic propellant expulsion systems.

References

[1] Saad, M. A. and DeBrock, S. C., "Simulation of Fluid Flow Phenomena in Propellant Tanks at High and Low Accelerations," *Journal of Spacecraft and Rockets*, Vol. 3, No. 12, Dec. 1966, pp. 1782–1788.

[2] Sloma, R. O., "Capillary Propellant Management System for Large Tank Orbital Propulsion Systems," *Proceedings of the 11th Liquid Propulsion Meeting*, Chemical Propulsion Information Agency Publication 190, Vol. II, Sept. 1969, pp. 53–66.

[3] Svenson, F. C., Simkin, D. J., and Field, R. E., "Apollo SPS Propellant Position Control in Low- and Zero-G Environments," SD-67-655, July 1967, North American-Rockwell Space Systems Div., Downey, Calif.

[4] De Brock, S. C., "Surface Tension Devices for Management of Space Propulsion System Propellants," *Proceedings, Society of Automotive Engineers Aerospace Systems Conference*, June 1967, pp. 230–236.

[5] DePeri, L. J., "A Resume of the Management of Liquid Gas Interface Using Surface Tension Technology," *Proceedings, Symposium on Low Gravity Propellant Orientation and Expulsion*, AIAA and Aerospace Corp., May 1968, pp. 75–84.

[6] De Brock, S. C., "Spacecraft Capillary Propellant Retention and Control for Long Life Missions," *Journal of Spacecraft and Rockets*, Vol. 6, No. 1, Jan. 1969, pp. 32–36.

[7] De Brock, S. C., "Development of a Capillary Propellant Management System for a Sixty-Two Inch Spherical Hydrazine Propellant Tank," *Proceedings, Symposium on Low Gravity Propellant Orientation and Expulsion*, AIAA and Aerospace Corp., May 1968, pp. 69–73.

[8] Trump, G. E., Forrester, A. T., and Barcatta, F. A., "Surface Tension Storage and Feed Systems for Ion Engines," AIAA Paper 66-249, San Diego, Calif., 1966.

[9] Worlock, R. M. et al., "An Advanced Contact Ion Microthruster System," *Journal of Spacecraft and Rockets*, Vol. 6, No. 4, April 1969, pp. 424–429.

[10] Hunter, R. E. et al., "Cesium Contact Ion Microthruster Experiment Aboard Applications Technology Satellite (ATS-IV)," *Journal of Spacecraft and Rockets*, Vol. 6, No. 9, Sept. 1969, pp. 968–70.

[11] Barber, H. W., "Negative-G Drone Aircraft Surface Tension Fuel System," AIAA Paper 70-910, Los Angeles, Calif., 1970.

[12] Satterlee, H. M. and Hollister, M. P., *Engineers Handbook: Low-G Propellant Behavior*, CR 92083, May 1967, NASA.

[13] Abramson, H. N., ed., *The Dynamic Behavior of Liquids in Moving Containers*, 1966, NASA, SP-106.

[14] Seebold, J. C., Hollister, M. P., and Satterlee, H. M., "Capillary Hydrostatics in Annular Tanks," *Journal of Spacecraft and Rockets*, Vol. 4, No. 1, Jan. 1967, pp. 101–105.

[15] Satterlee, H. M. and Chin, J. H., "Meniscus Shape Under Reduced Gravity Conditions," *Proceedings, Symposium on Fluid Mechanics and Heat Transfer Under Low Gravity Conditions*, U. S. Air Force Office of Scientific Research and Lockheed Aircraft Corp., 1965.

[16] Novozhilov, V. V., *Thin Shell Theory*, 2nd ed., P. Noordhoff, Groningen, Netherlands, 1964.

[17] Reynolds, W. C., Saad, M. A., and Satterlee, H. M., "Capil-

lary Hydrostatics and Hydrodynamics at Low-G," TR LG-3, Sept. 1964, Mechanical Engineering Dept., Stanford Univ., Palo Alto, Calif.

[18] Masica, W. J., "Experimental Investigation of Liquid Surface Motion in Response to Lateral Acceleration During Weightlessness," TN D-4066, July 1967, NASA.

[19] Beliaeva, M. A., Slobozhanin, L. A., and Tiuptsov, A. D., "Hydrostatics in Weak Force Fields," *Introduction to the Dynamics of Fluid-Containing Bodies Under Conditions of Weightlessness*, Moscow, Russia; also *Mathematical Methods to Dynamic Space Apparatus*, Vol. 6, 1968, pp. 5–68.

[20] Perko, L. M. and Moore, R. E., "Inviscid Fluid Flow in an Accelerating Cylindrical Container," *Journal of Fluid Mechanics*, Vol. 22, Pt. 2, June 1965, pp. 305–320.

[21] Concus, P., Crane, G. E., and Perko, L. M., "Inviscid Flow in an Accelerating Axisymmetric Container," *Proceedings, Symposium on Fluid Mechanics and Heat Transfer Under Gravity Conditions*, U.S. Air Force Office of Scientific Research and Lockheed Aircraft Corp., 1965.

[22] Burge, G. W., Blackmon, J. B., and Madsen, R. A., "Analytical Approaches for the Design of Orbital Refueling Systems," AIAA Paper 69-567, Colorado Springs, Colo., 1969.

[23] Labus, T. L. and Masica, W. J., "Liquid Reorientation in Spheres by Means of Low-G Accelerations," TM X-1659, Oct. 1968, NASA.

[24] Easton, C. R. and Catton, I., "Nonlinear Free-Surface Effects in Tank Draining at Low Gravity," AIAA Paper 69-680, San Francisco, Calif., 1969.

[25] Yeh, G. C. K. and Graham, D. J., "Draining of a Liquid from a Transversely Moving Cylindrical Tank," AIAA Paper 69-679, San Francisco, Calif., 1969.

[26] Gluck, D. F. et al., "Distortion of a Free Surface During Tank Discharge," *Journal of Spacecraft and Rockets*, Vol. 3, No. 11, Nov. 1966, pp. 1961–1962.

[27] Saad, M. A., "Free Surface Behavior During Propellant Withdrawal," *Proceedings, Symposium on Low Gravity Propellant Orientation and Expulsion*, AIAA and Aerospace Corp., May 1968, pp. 27–35.

[28] Sloma, R. O., "Surface Tension Techniques for Control of Propellant Free-Surface Behavior," *Proceedings, Symposium on Low Gravity Propellant Orientation and Expulsion*, AIAA and Aerospace Corp., May 1968.

[29] Kline, S. J., *Similitude and Approximation Theory*, McGraw-Hill, New York, 1965.

[30] Langhaar, H. L., *Dimensional Analysis and Theory of Models*, Wiley, New York, 1951.

[31] Lepper, R., "Northrop Space Laboratories Aero Gravity Simulation Facilities," *1963 Proceedings, Institute of Environmental Sciences Annual Technical Meeting*, 1963, pp. 461–464.

[32] Paynter, H. L., "The Martin Company's Low-G Experimental Facility," *Proceedings, Symposium on Fluid Mechanics and Heat Transfer Under Low Gravity Conditions*, U.S. Air Force Office of Scientific Research and Lockheed Aircraft Corp., 1965.

[33] Papell, S. S. and Faber, O. C., "Zero-Gravity and Reduced-Gravity Simulation on a Magnetic-Colloid Pool-Boiling System," TN D-3288, Feb. 1966, NASA.

[34] Clark, L. V. and Stephens, D. G., "Simulation and Scaling of Low-Gravity Slosh Frequencies and Damping," TM X-60484, Sept. 1967, NASA.

[35] Dodge, F. T., "A Discussion of Laboratory Methods of Simulating Low-Gravity Fluid Mechanics," TR 3, Feb. 1967, Southwest Research Institute, San Antonio, Texas.

[36] Saad, M. A. and Oliver, D. A., "Linearized Time Dependent Free Surface Flow in Rectangular and Cylindrical Tanks," *Proceedings, 1964 Heat Transfer and Fluid Mechanics Institute*, Stanford Univ. Press, Calif., 1964, pp. 81–99.

[37] Dodge, F. T. and Garza, L. R., "Experimental and Theoretical Studies of Liquid Sloshing at Simulated Low-Gravity," *Transactions of the ASME, Ser. E: Journal of Applied Mechanics*, Vol. 34, No. 3, Sept. 1967, pp. 555–562.

[38] Barksdale, T. R. and Paynter, H. L., "Design, Fabrication, and Testing of Subscale Propellant Tanks with Capillary Traps," CR-61676, 1968, NASA.

[39] Grubb, L. S. and Petrash, D. A., "Experimental Investigation of Interfacial Behavior Following Termination of Outflow in Weightlessness," TN D-3897, April 1967, NASA.

[40] Hollister, M. P., Satterlee, H. M., and Cohan, H., "A Study of Propellant Behavior During Periods of Varying Accelerations," CR-92084, June 1967, NASA.

[41] Toole, L. E. and Hastings, L. J., "An Experimental Study of the Behavior of a Sloshing Liquid Subjected to a Sudden Reduction in Acceleration," TM X-53755, Aug. 1968, NASA.

[42] Hastings, L. J., "Experimental Study of the Response of a Static Liquid Vapor Interface after a Sudden Reduction in Acceleration," TM X-53841, June 1969, NASA.

[43] Hollister, M. P., "Propellant Containment Utilizing Screen Mesh and Perforated Surfaces," A665481, Dec. 1964, Lockheed Missiles & Space Co., Sunnyvale, Calif.

[44] Jetter, R. I., "Orientation of Fluid Surfaces in Zero Gravity Through Surface Tension Effects," *Symposium on Physical and Biological Phenomena in a Weightless State*, American Astronautical Society, Los Angeles, Calif., 1963, Vol. 14, pp. 60–71.

[45] Abdalla, K. L. and Berenyi, S. G., "Vapor Ingestion Phenomenon in Weightlessness," TN D-5210, May 1969, NASA.

[46] Nussle, R. C., Derdul, J. D., and Petrash, D. A., "Photographic Study of Propellant Outflow from a Cylindrical Tank During Weightlessness," TN D-2572, Jan. 1965, NASA.

[47] Derdul, J. D., Grubb, L. S., and Petrash, D. A., "Experimental Investigation of Liquid Outflow from Cylindrical Tanks During Weightlessness," TN D-3746, Dec. 1966, NASA.

[48] Lubin, B. T and Hurwitz, M , "Vapor Pull-Through at a Tank Drain with and without Dielectrophoretic Baffling," Paper presented at Conference on Long-Term Cryo-Propellant Storage in Space, Oct. 12–13, 1966, Huntsville, Ala.

[49] Satterlee, H. M. and Reynolds, W. C., "The Dynamics of the Free Liquid Surface in Cylindrical Containers Under Strong Capillary and Weak Gravity Conditions," TR LG-2, May 1964, Mechanical Engineering Dept., Stanford Univ., Palo Alto, Calif.

[50] Bowman, T. E., "Liquid Settling in Large Tanks," *Proceedings, Symposium on Fluid Mechanics and Heat Transfer Under Low Gravity Conditions*, U.S. Air Force Office of Scientific Research and Lockheed Aircraft Corp., 1965.

[51] Bowman, T. E., "Response of the Free Surface on a Cylindrically Contained Liquid to Off-Axis Accelerations," *Proceedings, 1966 Heat Transfer and Fluid Mechanics Institute*, Stanford University Press, Calif., 1966, pp. 295–314.

[52] Salzman, J. A. and Masica, W. J., "Experimental Investigation of Liquid Propellant Reorientation," TN D-3789, Jan. 1967, NASA.

[53] Muraca, R. F., Whittick, J. S., and Neff, J. A., "Treatment of Metal Surfaces for Use with Space Storable Propellants: A Critical Survey," SR-951581-8, Aug. 1968, Stanford Research Institute, Palo Alto, Calif.

[54] Young, J. P., Reid, G. I., and Lamb, V. A., "Compatibility of Tank Coatings and Materials with Liquid Propellants," R-9960, Dec. 1968, National Bureau of Standards, Washington, D.C.

[55] Lorenz, P. M., "Compatibility of Tankage Materials with Liquid Propellants," AFML-TR-69-99, May 1969, The Boeing Co., Seattle, Wash.

[56] Salvinski, R. J., Howell, G. W., and Lee, D. H., "Advanced Valve Technology. Volume II, Materials Compatibility and Liquid Propellant Study," R-06641-601 4-R000, Nov. 1967, TRW Systems, Redondo Beach, Calif.

[57] Uney, P. E., "Compatibility of Storage Materials with Various Rocket Propellants," SR 1660-69-20, Nov. 1969, Martin Marietta Corp., Denver, Colo.

[58] Salvinski, R. J., "Investigation of the Formation and Behavior of Clogging Material in Earth and Space Storabe Propellants," R-08113-6025-R000, Nov. 1969, TRW Systems, Redondo Beach, Calif.

[59] Cain, E. F. C. et al, "Nitrogen Tetroxide Corrosion Products," R-7789, Feb. 1969, North American-Rockwell Corp., Rocketdyne Div., Cangoa Park, Calif.; also issued as AFR-PL-TR-69-114.

[60] Tartar, H. V., Sivertz, V., and Reitmeier, R. E., "The Surface Tension of Aqueous Solutions of Some Paraffin Chain Colloidal Electrolytes, including a Comparison of the Capillary Rise and Sessile Bubble Methods of Measurement," *Journal of the American Chemical Society*, Vol. 62, Sept. 1940, pp. 2375–2380.

[61] Muraca, R. F. and Whittick, J. S., "The Results of Long Term Shortage Tests for Compatibility of Nitrogen Tetroxide with Various Spacecraft Materials," SR-951581-2, May 1967, Stanford Research Institute, Palo Alto, Calif.

[62] Muraca, R. F., Whittick, J. S., and Crutchfield, C. A., "The Results of Long Term Storage Tests for Compatibilities of Spacecraft Materials with Hydrazine and Hydrazine Mixtures," SR-951581-6, Oct. 1967, Stanford Research Institute, Palo Alto, Calif.